

FOCAL-PLANE SCANNER FOR MEASURING RADOME BEAM DEFLECTION IN A COMPACT RANGE

Scott T. McBride

MI Technologies
1125 Satellite Blvd., Suite 100
Suwanee, GA 30024
smcbride@mi-technologies.com

ABSTRACT

Measurement of radome beam deflection and/or Boresight shift in a compact range generally requires a complicated set of positioner axes. One set of axes usually moves the radome about its system antenna while the system antenna remains aligned close to the range axis. Another set of axes is normally required to scan the system antenna through its main beam (or track the monopulse null) in each plane so the beam pointing angle can be determined. The fidelity required for the beam pointing angle, combined with the limited space inside the radome, usually make this antenna positioner difficult and expensive to build.

With a far-field range, a common approach to the measurement of beam deflection or Boresight shift uses a down-range X-Y scanner under the range antenna. By translating the range antenna, the incident field's angle of arrival is changed slightly. Because the X-Y position errors are approximately divided by the range length to yield errors in angle of arrival, the fidelity required of the X-Y scanner is not nearly as difficult to achieve as that of a gimbal positioner for the system antenna.

This paper discusses a compact-range positioner geometry that approximates the simplicity of the down-range-scanner approach commonly used on far-field radome ranges. The compact-range feed is mounted on a small X-Y scanner so that the feed aperture moves in a plane containing the reflector's focal point. Translation in this 'focal plane' has an effect very similar to the X-Y translation on a far-field range, altering the direction of arrival of the incident plane wave. Measured and modeled data are both presented.

Keywords: Beam Deflection, Boresight Shift, Compact Range, Focal-Plane Scanner, Measurement Systems, Radome

1. Introduction

When testing a radome that contains a moving antenna, testing of multiple antenna-to-radome aspects is required. Independent control of radome and system-antenna (the one inside the radome) motion is therefore needed in a test facility for such a radome. The testing of beam deflection generally requires scanning the antenna pattern through the peak region to determine the location of that peak. There are two options for adjusting the angle between the system antenna's pointing direction and the direction of the incident field:

- Rotate the system antenna relative to a fixed incident field. This requires a positioning system (typically a gimbal) for the system antenna. This positioning system might be mounted to a fixed post, or its mount might rotate in azimuth with the radome so that the antenna's positioner also counter-rotates the radome positioner.
- Rotate the incident field about a fixed antenna. This is easily done on a far-field range by using an X-Y scanner, where the direction of arrival (in radians) is approximately equal to the linear displacement over the range length.

Any designer of a radome-measurement facility must always be aware of the fidelity requirements, which tend to be extreme compared to the needs of a typical antenna-measurement system. Transmission efficiency fidelity (either repeatability or accuracy) is typically specified to be better than 1% or 2% power, which corresponds to 0.04 and 0.08 dB, respectively. Deflection of a monopulse null often requires system-level fidelity of a tenth of a milliradian, or 0.0057°. The small size, counter-steering dynamics, large range of motion, and handling of RF cabling to the system antenna make these requirements very difficult to meet using a gimbal under the system antenna.

MI Technologies (MI) has successfully built gimbal-based radome facilities that meet these demanding requirements [1-3]. Each, however, required significant integration time to achieve the required performance. For a new low-cost,

low-volume, high-fidelity facility at MI, we needed a solution with low integration risk. MI had conceived the geometry of the 'focal-plane scanner' in an internal look at gimbal alternatives, and felt that it was the best concept to meet the constraints of the new facility.

The 'focal-plane scanner' as defined herein is a tilted X-Y scanner that moves the compact-range feed in a plane that includes the reflector's focal point. Figure 1 below illustrates this scanner geometry. Note in Figure 1 that the X and Y axes represent the DUT coordinate system, while the X' and Y' axes have been translated and then rotated about X' to be normal to the feed's longitudinal axis.

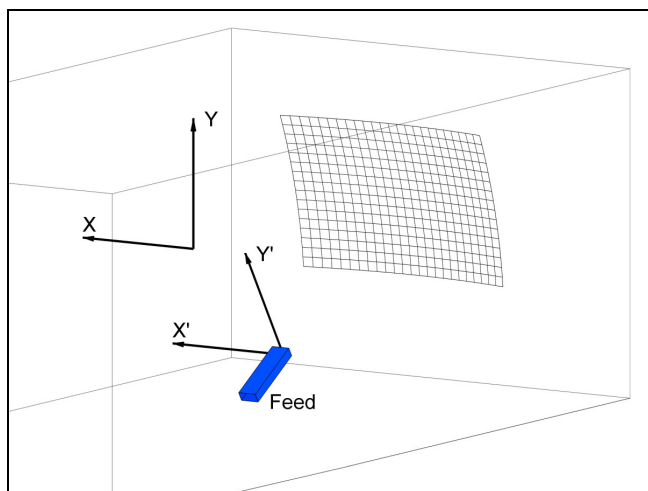


Figure 1 – Focal-Plane Scanner Geometry

The purpose of the focal-plane scanner is to change the direction of arrival of the plane wave incident on a stationary system antenna, much the same as a down-range X-Y scanner does in a far-field geometry. This paper describes a functioning radome measurement facility that employs a focal-plane scanner in a compact range.

2. History

The technique of changing the primary plane wave's direction by moving the feed off a reflector's focal point is not new. It has been used extensively in the design of reflector antennas [4]. The fundamental principles of this technique have also been previously used in compact ranges for antenna and/or radome measurements [5-7]. This is, however, the first known application of a focal-plane scanning technique to radome measurements in a compact range.

3. Basic Theory

The paraboloidal shape is used for single-reflector compact-ranges because it transforms the feed's spherical wave to a plane wave incident on the device under test (DUT). This

transformation is only pure for an infinitely large paraboloid, and with an ideal feed located at the focal point. Small feed translations along X' and/or Y' approximate a plane wave arriving from a different direction, as illustrated in Figure 2 below. This approximation gets worse with increasing distance from the focal point. The nature of the degradation is a lack of planarity in the phase front, and is depicted in Figure 3 and discussed below. If this distortion, combined with the other non-ideal conditions in the test facility, is still within the established tolerances of compact-range phase planarity, then it does not represent a problem.

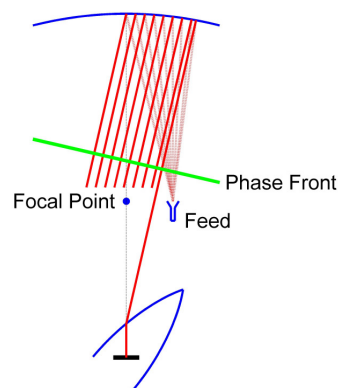


Figure 2 –Off-Axis Parabola Characteristics

Figure 2 illustrates (viewed from above, and using an exaggerated deflection) several things about the geometry of interest. The system antenna (inside the radome) is always pointed toward the center of the reflector. We will assume in this paragraph that it is transmitting, but that is not required. When the RF field passes through the radome, it may be deflected to a different direction, then it propagates toward the reflector, and finally bounces back toward the feed location shown in Figure 2.

A reflector's transformation between spherical and plane waves is primarily a result of path lengths, not of ray tracing. For an ideal parabola, however, the result is the same using either approach. Let us now assume that the feed has been offset (as shown) to intercept the one ray shown coming from the radome. If we then draw several rays from the feed toward the reflector (also as shown), all of them are reflected roughly parallel to each other and to the ray from the radome. If we draw a contour (shown in green above) through the different rays at equal path length, it will be very close to a straight line normal to the individual rays. To the extent that the phase front resembles a straight line (or flat plane in 3D), the compact range is still producing (or responding to) a single plane wave. This

single plane wave's direction of arrival is determined by the location of the feed.

If we were to look extremely closely at the seemingly parallel red lines originating at the feed in Figure 2, we would see that they are not quite parallel. The green phase front of the offset feed is also not quite linear. Similarly, if we were to illuminate the reflector with an ideal off-axis plane wave, the reflected rays would not converge at a single feed location. When the deflection is small, the rays all come very close to a single point, but the convergence degrades as the deflection gets larger. Radome beam deflection is usually much less than one degree ($\ll 17$ mrad), so all the necessary deflections on the focal-plane scanner (as well as the corresponding phase distortions) are very small.

4. Findings

If the compact-range reflector were a symmetric (centered) paraboloid, the logical locus of points for the feed would lie close to a vertical plane through the focal point. However, there is no reason to minimize the error on the missing bottom half of the paraboloid, but instead the errors ought to be made somewhat symmetric about the center of the reflector. Extensive modeling verified that the least quiet-zone distortion resulted from feed travel near a plane normal to the feed's pointing angle.

We expected the feed to require motion along its longitudinal (Z') axis as it translated in X' and/or Y' away from the focal point. For the small deflections needed in this facility, motion in the plane normal to the feed's longitudinal axis yielded adequate performance.

The phase distortion that results from displacing the feed in X' and Y' is shown in Figure 3 below. This figure represents modeled data, and is the deviation from the best-fit plane of the phase that might be measured by an X-Y scanner located in the quiet zone. The axis along the bottom of Figure 3 is phase, and ranges from -0.9° to $+0.6^\circ$ in the geometry modeled. The other two axes represent the X and Y quiet-zone axes shown in Figure 1 above. The model was run for this example at 15 GHz, with the feed displaced in both X' and Y' by 2.6". The path length from the feed to each point in the quiet zone is fixed for a particular set of X' - Y' displacements, so the phase distortion depends upon the wavelength while the direction of arrival remains constant with frequency.

One can observe in Figure 3 that the worst phase distortion occurs off axis in both X and Y (in the quiet zone). The common practice of collecting field-probe data only in horizontal and vertical cuts may therefore underestimate the phase distortion. The 45° roll angles (on a probe-slide-

over-roll-over-az positioner) are generally sufficient to capture the worst expected distortion.

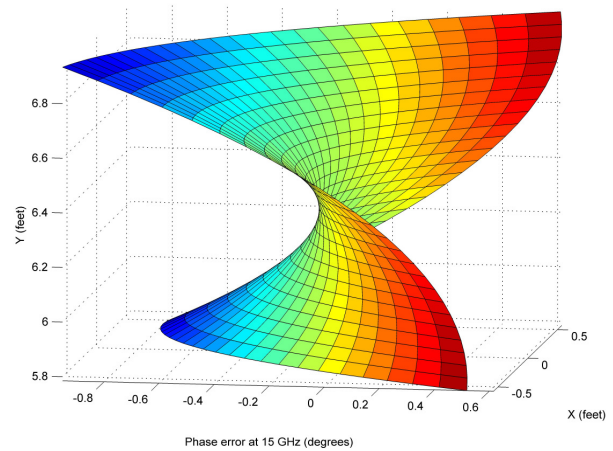


Figure 3 – Modeled Deviation of Quiet-Zone Phase From a Plane Wave When Feed is Offset

A coarse estimate of the azimuth direction of plane-wave arrival as a function of the feed displacement X' would be given by $Az \approx \tan^{-1}(X'/F)$, where F is the focal length of the compact-range reflector. For the small deflections ($< 4''$ vs. a focal length F of 144"), we can further approximate $Az \approx X'/F$ (in radians). A similar coarse relationship would hold for elevation direction as a function of Y' feed translation. A more accurate version of this characterization was made by running the model with several X' and/or Y' feed displacements, then examining the best-fit plane to find azimuth and elevation pointing directions. The results of these simulations were evaluated, and fit with curves of the form:

$$Az = C_1X' + C_2Y'$$

$$El = C_3Y' + C_4X' + C_5Y'^2 + C_6X'^2$$

The dominant term in each equation is very similar to the coarse estimate above. The extra terms, however, are needed to obtain the required accuracy. Note that azimuth and elevation angular deflections are each a function of both X' and Y' feed deflections.

5. Implementation

In order to test the radomes of interest in this facility, we needed scanner travel of about 7" by 7". However, we already had available a very high-quality 36" by 36" planar near-field scanner. A wedge was used to tilt the entire scanner structure back to the normal 32° feed pointing angle. A plywood-backed absorber fence was built in front of the scanner with an 8" by 8" hole in the fence surrounding the feed. The tilted scanner is visible in Figure

4. The feed protrudes through the absorber on the fence, as shown in Figure 5, and another piece of absorber mounted on the moving feed covers the hole in the fence for all feed X' and Y' travel.



Figure 4 – Rear View of Focal-Plane Scanner

There was concern that the mutual coupling from this large metallic structure near the focal point would cause a problem. As demonstrated by measured field probe data, however, the absorber treatment shown in Figure 5 was sufficient to overcome this concern.

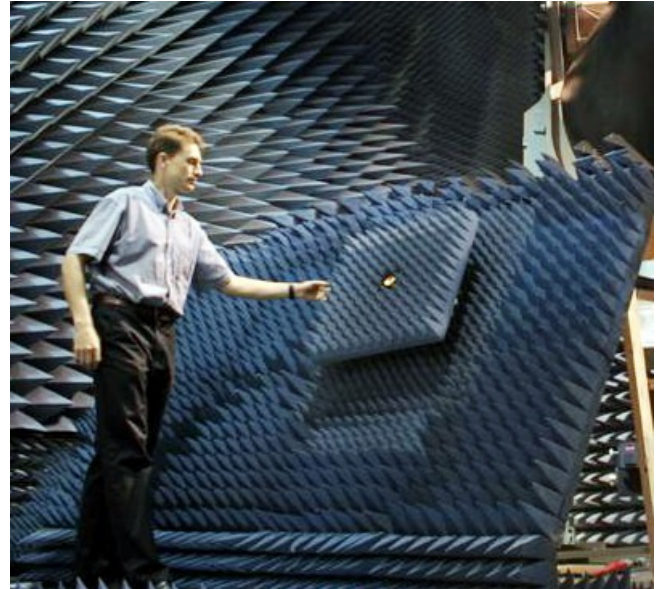


Figure 5 – Focal-Plane Scanner Absorber Treatment

6. Results

The beam-deflection and Boresight-shift accuracy of the facility was demonstrated as follows:

- Align the system antenna close to the range axis
- Measure the optical and RF pointing direction
 - Measure the system antenna's optical pointing angles with an autocollimating theodolite
 - Determine the az-el pointing direction of the system antenna from RF data
- Intentionally misalign the system antenna to point somewhere in the range of expected beam deflections
- Measure the optical and RF pointing direction, and compare to the readings with the system antenna aligned near the range axis
- Repeat the two steps above several times.
- Plot the difference between optical and RF deflection vs. the optical deflection

Figure 6 below shows the measured azimuth beam deflection accuracy for one of the system antennas. The optical deflection from the process above is assumed to be the correct answer. The accuracy required for sum-beam deflection in the azimuth plane was fairly coarse, and the system was easily within that specification, with less than 0.3 mrad of error through 9 mrad of deflection.

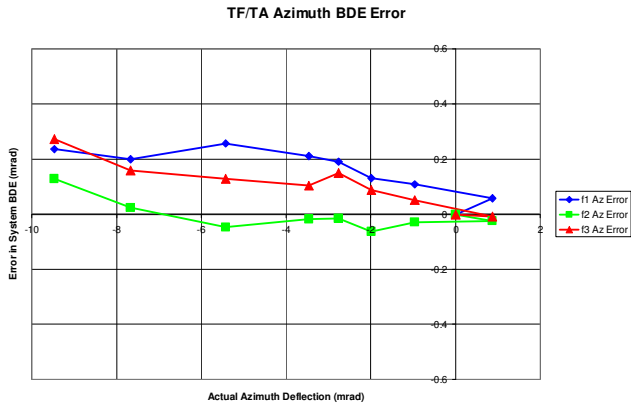


Figure 6 – Error Between RF and Optical Determination of Azimuth Beam Deflection

Figure 7 below shows the measured elevation Boresight shift accuracy (measured using a monopulse system antenna). Note that the overall slope (and some of the bow) in Figure 7 could have been removed by adjusting the coefficients that convert between X'-Y' translation and elevation deflection, but the data shown were already within specifications.

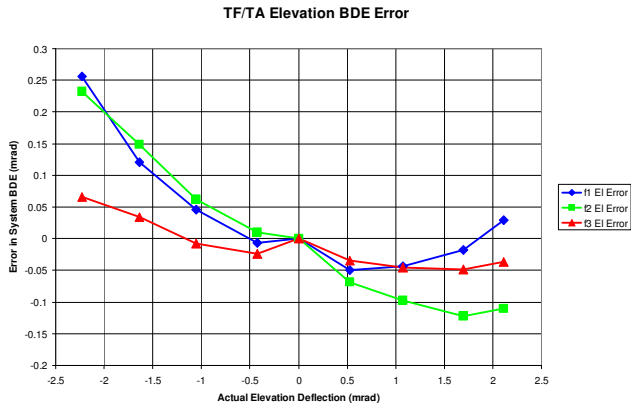


Figure 7 – Error Between RF and Optical Determination of Elevation Boresight Shift

Figure 8 below shows one example of beam deflection measured in the radome test facility. The colors represent small sum beam deflections at Ka band for multiple radome azimuth, elevation, and roll angles. An az-el surface plot is warped to the radome surface (represented by the large translucent shape) at each of the three roll angles. Note the continuity among the radome roll angles of the beam deflection caused by the radome. Examination of the radome using this plot confirmed that repairs had been made at the locations indicated. Figure 9 below shows a similar plot for X-band data on the same radome.

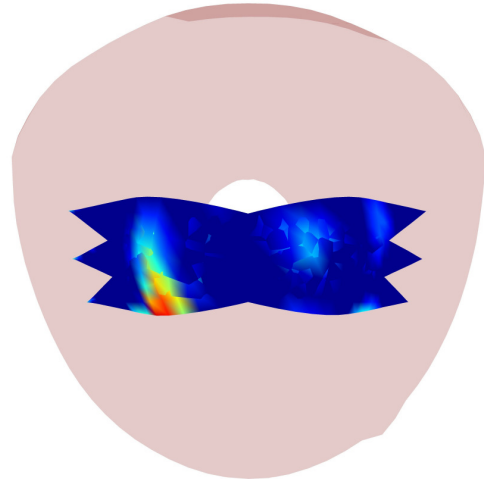


Figure 8 – Measured Ka-Band Beam Deflection Data Mapped To Radome Surface

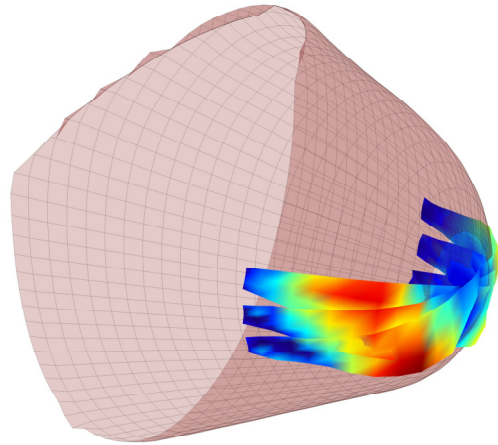


Figure 9 – Measured X-Band Beam Deflection Data Mapped To Radome Surface

7. Conclusions

MI's initial implementation of a focal-plane scanner was completely successful. We were easily able to achieve both the transmission-efficiency and beam-deflection accuracy specifications for the facility, and this has proven difficult in other radome systems when using a gimbal-based positioning system. Beam-deflection accuracy (not merely repeatability) of better than 0.3 mrad was achieved without any unplanned corrections or compensations. This technique combines the advantages of the compact-range configuration and the down-range X-Y scanner geometry. While there is no single 'ideal radome test configuration', the focal-plane scanner configuration has distinct advantages for those situations where it is applicable.

8. References

- [1] Hudgens, J.M., and Cawthon, G.M., "Extreme Accuracy Tracking Gimbal for Radome Measurements", Proc AMTA '03, Irvine, CA, pp. 291-295.
- [2] McBride, S.T., and Cawthon, G.M., "Error Compensation for Radome Measurements", Proc AMTA '04, Atlanta, GA, pp. 502-507.
- [3] McBride, S.T., and Musser, D.J., "Results of a New RF Cable Correction Method", Proc AMTA '06, Austin, TX, pp. 266-270.
- [4] Volakis, J.L., Antenna Engineering Handbook, fourth edition, McGraw Hill, 2007, Chapter 15.
- [5] Jones, J.R., Hess, D.W., Jory, V., Smith, D., and Folsom, D.M., "System Engineering for a Radome Test System", Proc AMTA '94, Long Beach, CA, pp. 111-116.
- [6] Jory, V., Jones, J.R., Farr, V., Manning, S.J., Oh, L.L., Pearson, G.W., and Norin, T.L., "Triband Radome Measurement System: Installation and Testing Results", Proc AMTA '95, Williamsburg, VA, pp. 276-281.
- [7] Viikari, V., Häkli, J., Ala-Laurinaho, J., Mallat, J., and Räisänen, A.V., "A Feed Scanning Based APC-Technique for Improving the Measurement Accuracy in a Sub-MM CATR", Proc AMTA '04, Atlanta, GA, pp. 227-231.